Journal of Sound and Vibration (2002) **253**(5), 985–1000
doi:10.1006/jsvi.2001.3974, available online at http://www.idealibrary.com on IDEAL®

RESONANCES OF A NON-LINEAR s.d.o.f. SYSTEM WITH TWO TIME-DELAYS IN LINEAR FEEDBACK CONTROL

J. C. Ji

Department of Mechanical Engineering, Baotou University of Iron and Steel Technology, Baotou 014010, *Inner Mongolia, People's Republic of China. E-mail*: *jchji2@hotmail.com*

AND

A. Y. T. Leung

Department of Building and Construction, City University of Hong Kong, Kowloon, Hong Kong

(*Received* 19 *October* 2000, *and in final form* 29 *May* 2001)

The primary, superharmonic, and subharmonic resonances of a harmonically excited non-linear s.d.o.f. system with two distinct time-delays in the linear state feeback are studied. The two different time-delays are presented in the proportional feedback and the derivative feedback respectively. The method of multiple scales is utilized to obtain the first order approximation of response. The effect of the feedback gains and time-delays on the steady state responses of three types of resonances is investigated. It is found that a proper selection of the feedback gains and time-delays can enhance the control performance.

1. INTRODUCTION

Time-delays, which are especially prevalent if a digital control system is being implemented, can limit the performance of the feedback controllers in practical mechanical or structural systems [1]. The addition of such unavoidable time-delays in the feedback path not only causes the transfer function of the controller to be modified, but may also induce the instability of the controlled system. On the other hand, the time-delays can deliberately be implemented to achieve better system behavior when control is applied with the time-delays [2]. The effect of the feedback gains and time-delays on the dynamical behavior of the controlled system is thus required to be investigated for the design of optimal controllers.

The non-linear system with the time-delays has been an active topic of research over the past decades [3–6]. Plaut and Hsieh [3] numerically analyzed the steady response of a non-linear one-degree-of-freedom mechanism with the time-delays for various sets of parameters, by a Runge–Kutta numerical integration procedure. It was found that the response might be periodic, chaotic or unbounded. By the method of multiple scales, Plaut and Hsieh [4] studied the effect of a damping time-delay on non-linear structural vibrations and analyzed six resonance conditions. They gave the results in a number of figures for the steady state response amplitude versus the excitation frequency and amplitude. Moiola *et al.* [5] investigated the degeneracy conditions of Hopf bifurcation in an autonomous non-linear feedback system with the time-delay using the frequency–domain approach. Two simple examples of non-linear autonomous delayed systems were presented. The computation of the two periodic branches near a degenerate Hopf bifurcation point was given. Hu *et al.* [6] studied the primary and subharmonic resonances of a harmonically forced Duffing oscillator with two identical time-delays in the state feedback. The concept of an equivalent damping was proposed, and an appropriate choice of the feedback gains and time-delay was discussed from the viewpoint of vibration control.

All of the aforementioned studies dealt with one time-delay or two identical time-delays in the state feedback terms. To the authors' knowledge, the complicated dynamical behavior of non-linear delayed systems with two distinct time-delays has received less attention, although the stability analysis of a linear s.d.o.f. system with two different time-delays has been documented [7].

In this paper, the non-linear dynamical behavior of a harmonically excited non-linear single-degree-of-freedom (s.d.o.f.) system with two distinct time-delays is analyzed under primary, superharmonic and subharmonic resonance conditions. Two time-delays occur in the proportional and derivative feedback. The equation of motion is assumed to have the following form:

$$\ddot{u} + \omega^2 u + \varepsilon(2\mu\dot{u} + \alpha u^3) = K\cos\Omega t + \varepsilon 2[g_p u(t-\tau_1) + g_d\dot{u}(t-\tau_2)]. \tag{1}$$

This system is related to the simplest model for many practical controlled systems, such as active vehicle suspension systems when the non-linearity in the tires is considered [8]. In equation (1), the damping, non-linearity and feedback gains are assumed to be small and of the same order. In the remainder of this paper, the method of multiple scales [9] is applied to equation (1) and three resonance conditions are examined. Attention here is focused on the effect of the time-delays and feedback gains on the steady state response. It is believed that the result will be of value in the design of optimal controllers for this general non-linear s.d.o.f. system.

2. FORMULATION AND ANALYSIS

2.1. PRIMARY RESONANCE

For the case of primary resonance, the excitation amplitude and frequency are such that

$$K = \varepsilon 2f, \quad \Omega = \omega + \varepsilon\sigma. \tag{2}$$

Using the method of multiple scales [9], one assumes an approximate solution of equation (1) in the form

$$u(t;\varepsilon) = u_0(T_0, T_1) + \varepsilon u_1(T_0, T_1) + \cdots, \tag{3}$$

where $T_n = \varepsilon^n t$, $n = 0, 1, 2, \ldots$.

Substituting equation (3) into equation (1) and equating the coefficients of like powers of ε, one has the following equations to order $O(1)$ and to order $O(\varepsilon)$:

$$D_0^2 u_0 + \omega^2 u_0 = 0,$$

$$D_0^2 u_1 + \omega^2 u_1 = -2D_0D_1u_0 - 2\mu D_0 u_0 - \alpha u_0^3 - 2f\cos\Omega t + 2g_p u_0(t-\tau_1) + 2g_d\dot{u}_0(t-\tau_2), \tag{4}$$

where $D_n = \partial/\partial T_n$, $n = 0, 1, 2, \ldots$. A first order approximate solution of equation (1) can be written as

$$u = a\cos(\Omega t - \gamma) + O(\varepsilon). \tag{5}$$

The amplitude a and phase γ of the response is governed by the following polar form of modulation equations:

$$a' = -\left(\mu + \frac{g_p}{\omega}\sin\omega\tau_1 - g_d\cos\omega\tau_2\right)a + \frac{f}{\omega}\sin\gamma,$$

$$a\gamma' = \left(\sigma + \frac{g_p}{\omega}\cos\omega\tau_1 + g_d\sin\omega\tau_2\right)a - \frac{3\alpha}{8\omega}a^3 + \frac{f}{\omega}\cos\gamma, \tag{6}$$

where a prime indicates the derivative with respect to the time scale T_1. Obviously, the presence of the feedback gains and time-delays modifies the averaged equations by adding two terms that are relevant to feedback control. Thus, it is possible to achieve the desirable behavior if the feedback is deliberately implemented.

Steady state solutions of equation (1) for the primary resonance response correspond to the fixed points of equation (6), which can be obtained by setting $a' = \gamma' = 0$. That is,

$$-\left(\mu + \frac{g_p}{\omega}\sin\omega\tau_1 - g_d\cos\omega\tau_2\right)a + \frac{f}{\omega}\sin\gamma = 0,$$

$$\left(\sigma + \frac{g_p}{\omega}\cos\omega\tau_1 + g_d\sin\omega\tau_2\right)a - \frac{3\alpha}{8\omega}a^3 + \frac{f}{\omega}\cos\gamma = 0. \tag{7}$$

From equation (7), the so-called frequency–response equation is obtained:

$$\left[\mu_e^2 + \left(\sigma_e - \frac{3\alpha}{8\omega}a^2\right)^2\right]a^2 = \left(\frac{f}{\omega}\right)^2, \tag{8}$$

where

$$\mu_e = \mu + \frac{g_p}{\omega}\sin\omega\tau_1 - g_d\cos\omega\tau_2, \quad \sigma_e = \sigma + \frac{g_p}{\omega}\cos\omega\tau_1 + g_d\sin\omega\tau_2.$$

The amplitude of the response is a function of the external detuning, feedback gains, time-delays and the amplitude of the excitation.

The peak amplitude of the primary resonance response, obtained from equation (8), is given by

$$a_p = \frac{f}{\omega\mu_e}. \tag{9}$$

The real solution a of equation (8) determines the primary resonance response amplitude. There can be either one or three real solutions. Three real solutions exist between two points of vertical tangents (saddle–node bifurcation) [10, 11], which are determined by differentiation of equation (8) implicitly with respect to a^2. This leads to the condition

$$\sigma_e^2 - \frac{3\alpha}{2\omega}a^2\sigma_e + \frac{27\alpha^2}{64\omega^2}a^4 + \mu_e^2 = 0 \tag{10}$$

with solutions

$$\sigma_e^{\pm} = \frac{3\alpha}{4\omega}a^2 \pm \left(\frac{9\alpha^2}{64\omega^2}a^4 - \mu_e^2\right)^{1/2}. \tag{11}$$

For $(3|\alpha|/8\omega)\,a^2 > \mu_e$, there exists an interval $\sigma_e^- < \sigma_e < \sigma_e^+$ in which three real and positive solutions a of equation (8) exist. In the limit $(3|\alpha|/8\omega)\,a^2 \to \mu_e$, this interval shrinks to the point $\sigma_e = (3\alpha/4\omega)\,a^2$. The critical force amplitude obtained from equation (8) is

$$f_{crit} = 4\omega\mu_e[\mu_e\omega/(3|\alpha|)]^{1/2}. \tag{12}$$

For $f < f_{crit}$ there is only one solution while for $f > f_{crit}$ there are three. The stability of the solutions is determined by the eigenvalues of the corresponding Jacobian matrix of equation (6). The corresponding eigenvalues are the roots of

$$\lambda^2 + 2\mu_e\lambda + \mu_e^2 + \left(\sigma_e - \frac{3\alpha a^2}{8\omega}\right)\left(\sigma_e - \frac{9\alpha a^2}{8\omega}\right) = 0. \tag{13}$$

It turns out that the sum of the two eigenvalues is $-2\mu_e$. For the uncontrolled system, the sum of the two eigenvalues is -2μ, which is negative [10, 11]. The addition of the feedback gains and time-delays varies the sum of the two eigenvalues. Three cases such as $\mu_e > 0{\cdot}0$, $= 0{\cdot}0$ and $< 0{\cdot}0$ may occur depending on the values of the feedback gains and time-delays. If the feedback gains and time-delays are chosen in such a way that the sum of the two eigenvalues is positive ($\mu_e < 0$), at least one of the two eigenvalues will always have a positive real part. The system will be unstable. The selection of the feedback gains and time-delays is not possible. On the other hand, if the sum of the two eigenvalues is zero ($\mu_e = 0$) by a certain value of the feedback gains and time-delays, a pair of purely imaginary eigenvalues and hence a Hopf bifurcation may occur. Anyhow, the above two cases should be avoided from the viewpoint of bifurcation control. The feedback should be implemented at least in such a way that $\mu_e > 0$ is guaranteed. Under such feedback gains and time-delays, the sum of the two eigenvalues is always negative, and accordingly, at least one of the two eigenvalues will always have a negative real part. The other eigenvalue is zero when

$$\mu_e^2 + \left(\sigma_e - \frac{3\alpha a^2}{8\omega}\right)\left(\sigma_e - \frac{9\alpha a^2}{8\omega}\right) = 0, \tag{14}$$

where a saddle–node bifurcation occurs.

It has been shown that the feedback gains and time-delays can change the quantities of μ_e and σ_e, which govern the critical force amplitude, the peak amplitude of the primary resonance response, and the stability of steady state motions. The critical force amplitude f_{crit} is directly proportional to $\mu_e^{3/2}$, while the peak amplitude of the response a_p is inversely proportional to μ_e. Thus, the critical force f_{crit} increases (or decreases) while the peak amplitude of the response a_p decreases (or increases) as μ_e increases (or decreases). On the other hand, if the resulting μ_e and σ_e satisfy the inequality $\mu_e^2 + (\sigma_e - 3\alpha a^2/8\omega)(\sigma_e - 9\alpha a^2/8\omega) > 0$, no unstable solutions exist. The system will not exhibit jump and hysteresis phenomenon. Thus, the appropriate feeback gains and time-delays can enhance the control performance.

2.2. SUPERHARMONIC RESONANCE

To analyze the superharmonic resonance, the amplitude and frequency of excitation are expressed as

$$K = 2f, \quad 3\Omega = \omega + \varepsilon\sigma. \tag{15}$$

Using the method of multiple scales, one obtains the first order approximation for the superharmonic resonance response

$$u = a\cos(3\Omega t - \gamma) + 2f(\omega^2 - \Omega^2)^{-1}\cos\Omega t + O(\varepsilon), \tag{16}$$

where the amplitude a and phase γ of the free oscillation term are governed by

$$a' = -\mu_e a - \frac{\alpha\Lambda^3}{\omega}\sin\gamma,$$

$$a\gamma' = \left(\sigma_e - \frac{3\alpha\Lambda^2}{\omega}\right)a - \frac{3\alpha}{8\omega}a^3 - \frac{\alpha\Lambda^3}{\omega}\cos\gamma, \tag{17}$$

where $\Lambda = f(\omega^2 - \Omega^2)^{-1}$.

The fixed points of this system are given by

$$-\mu_e a - \frac{\alpha\Lambda^3}{\omega}\sin\gamma = 0,$$

$$\left(\sigma_e - \frac{3\alpha\Lambda^2}{\omega}\right)a - \frac{3\alpha}{8\omega}a^3 - \frac{\alpha\Lambda^3}{\omega}\cos\gamma = 0. \tag{18}$$

Squaring and adding these equations, one has the frequency–response equation

$$\left[\mu_e^2 + \left(\sigma_e - \frac{3\alpha\Lambda^2}{\omega} - \frac{3\alpha}{8\omega}a^2\right)^2\right]a^2 = \frac{\alpha^2\Lambda^6}{\omega^2}. \tag{19}$$

There can be one or three real solutions for the amplitude of superharmonic resonance response a. Saddle–node bifurcation occurs at

$$\sigma_e^{\pm} = \frac{3\alpha\Lambda^2}{\omega} + \frac{3\alpha}{4\omega}a^2 \pm \left(\frac{9\alpha^2}{64\omega^2}a^4 - \mu_e^2\right)^{1/2}. \tag{20}$$

For $(3|\alpha|/8\omega)a^2 > \mu_e$, there exists an interval $\sigma_e^- < \sigma_e < \sigma_e^+$ in which three real and positive solutions a of equation (19) exist. In the limit $(3|\alpha|/8\omega)a^2 \to \mu_e$, this interval shrinks to the point $\sigma_e = 3\alpha\Lambda^2/\omega + (3\alpha/4\omega)a^2$. The critical force amplitude obtained from equation (19) is

$$f_{crit} = (\omega^2 - \Omega^2)[16\mu_e^3\omega^3/(3|\alpha|^3)]^{1/6}. \tag{21}$$

For $f < f_{crit}$ there is only one solution while for $f > f_{crit}$ there are three. The critical force amplitude is directly proportional to $\mu_e^{1/2}$. Increasing μ_e can enlarge the value of f_{crit}.

The peak amplitude of the free oscillation term is given by

$$a_p = \frac{|\alpha|\Lambda^3}{\omega\mu_e}, \tag{22}$$

which is also inversely proportional to μ_e. Increasing μ_e can diminish the value of a_p.

The stability of the steady state superharmonic resonance response is determined by the eigenvalues of the corresponding Jacobian matrix, which are the roots of

$$\lambda^2 + 2\mu_e\lambda + \mu_e^2 + \left(\sigma_e - \frac{3\alpha\Lambda^2}{\omega} - \frac{3\alpha}{8\omega}a^2\right)\left(\sigma_e - \frac{3\alpha\Lambda^2}{\omega} - \frac{9\alpha}{8\omega}a^2\right) = 0. \tag{23}$$

The steady state motions are stable only when the two inequalities $\mu_e > 0$ and $\mu_e^2 + (\sigma_e - 3\alpha\Lambda^2/\omega - (3\alpha/8\omega)a^2)(\sigma_e - 3\alpha\Lambda^2/\omega - (9\alpha/8\omega)a^2) > 0$ simultaneously hold, and are otherwise unstable. The violation of the second condition would imply the existence of an eigenvalue having a positive real part. Replacing the inequality by an equality yields the critical parameters corresponding to saddle–node bifurcation. The suitable choice of the feedback gains and time-delays can improve the control performance. Moreover, the occurrence of saddle–node bifurcation, the jump and hysteresis phenomena can be delayed or eliminated.

2.3. SUBHARMONIC RESONANCE

For the case of subharmonic resonance, it is assumed that $K = 2f$ and $\Omega = 3\omega + \varepsilon\sigma$. The first order approximation for the steady state subharmonic resonance response is given by

$$u = a\cos[\tfrac{1}{3}(\Omega t - \gamma)] + 2f(\omega^2 - \Omega^2)^{-1}\cos\Omega t + O(\varepsilon), \tag{24}$$

where a and γ are governed by

$$a' = -\mu_e a - \frac{3\alpha\Lambda}{4\omega}a^2\sin\gamma,$$

$$a\gamma' = \left(\sigma_e - \frac{9\alpha\Lambda^2}{\omega}\right)a - \frac{9\alpha}{8\omega}a^3 - \frac{9\alpha\Lambda}{4\omega}a^2\cos\gamma, \tag{25}$$

where $\Lambda = f(\omega^2 - \Omega^2)^{-1}$.

The steady state response corresponds to the solutions of

$$-\mu_e a - \frac{3\alpha\Lambda}{4\omega}a^2\sin\gamma = 0,$$

$$\left(\sigma_e - \frac{9\alpha\Lambda^2}{\omega}\right)a - \frac{9\alpha}{8\omega}a^3 - \frac{9\alpha\Lambda}{4\omega}a^2\cos\gamma = 0. \tag{26}$$

Eliminating γ from these equations, one has the frequency–response equation

$$\left[9\mu_e^2 + \left(\sigma_e - \frac{9\alpha\Lambda^2}{\omega} - \frac{9\alpha}{8\omega}a^2\right)^2\right]a^2 = \frac{81\alpha^2\Lambda^2}{16\omega^2}a^4. \tag{27}$$

There are two possibilities: either a trivial solution $a = 0$, or non-trivial solutions, which are given by

$$9\mu_e^2 + \left(\sigma_e - \frac{9\alpha\Lambda^2}{\omega} - \frac{9\alpha}{8\omega}a^2\right)^2 = \frac{81\alpha^2\Lambda^2}{16\omega^2}a^2. \tag{28}$$

Its solutions are

$$a^2 = p \pm (p^2 - q)^{1/2}, \tag{29}$$

where

$$p = \frac{8\omega}{9\alpha}\sigma_e - 6\Lambda^2, \quad q = \frac{64\omega^2}{81\alpha^2}\left[9\mu_e^2 + \left(\sigma_e - \frac{9\alpha\Lambda^2}{\omega}\right)^2\right].$$

The non-trivial free-oscillation amplitudes occur only when $p > 0$ and $p^2 \geqslant q$ as q is always positive. These conditions demand that

$$\Lambda^2 < \frac{4\omega\sigma_e}{27\alpha}, \quad \text{and} \quad 8\omega\Lambda^2\alpha\sigma_e - 16\omega^2\mu_e^2 - 63\alpha^2\Lambda^4 \geqslant 0. \tag{30}$$

It follows that $\alpha\sigma_e$ must be at least non-negative.

The steady state solutions of subharmonic resonance response is determined by the eigenvalues of the characteristic equation, which are the roots of

$$\lambda^2 + 2\mu_e\lambda + \frac{27\alpha^2}{32\omega^2}a^2(a^2 - p) = 0. \tag{31}$$

It is noted that if the feedback control is appropriately implemented violating one of the two inequalities (30), the system will not exhibit subharmonic resonance. In other words, subharmonic resonance response can be eliminated by a proper feedback.

3. CASE STUDY

Based on the foregoing discussion, it can be concluded that the appropriate time-delays can improve the control performance. A certain combination of μ_e and σ_e can delay or eliminate the occurrence of saddle–node bifurcation in the primary and superharmonic resonance responses. Moreover, subharmonic resonance can be prevented from occurring in the controlled system, by a suitable feedback control. In this section, the effect of the feedback gains and time-delays on the quantities μ_e and σ_e will be discussed. Whenever numerical simulations are performed, the values for the system parameters are chosen as follows: $\alpha = 1{\cdot}0$, $\omega = 3{\cdot}0$, $\mu = 0{\cdot}05$, $f = 0{\cdot}27$, $g_p = 0{\cdot}09$, $g_d = 0{\cdot}01$, unless otherwise specified.

For simplicity, one expresses the time-delays in the form $\tau_1 = \tau$ and $\tau_2 = \phi + \tau_1 = \phi + \tau$. The parameters μ_e and σ_e become

$$\mu_e = \mu + \frac{g_p}{\omega}\sin\omega\tau - g_d\cos\omega(\phi + \tau),$$

$$\sigma_e = \sigma + \frac{g_p}{\omega}\cos\omega\tau + g_d\sin\omega(\phi + \tau). \tag{32}$$

Let

$$\frac{d\mu_e}{d\tau} = g_p\cos\omega\tau + \omega g_d\sin\omega(\phi + \tau) = 0,$$

$$\frac{d\sigma_e}{d\tau} = -g_p\sin\omega\tau + \omega g_d\cos\omega(\phi + \tau) = 0 \tag{33}$$

the difference of the two time-delays ϕ admits the following two solutions:

$$\phi = \frac{\pi}{2\omega} \quad \text{and} \quad \phi = \frac{3\pi}{2\omega} \tag{34}$$

at which μ_e and σ_e are

$$\mu_e = \mu + \left(\frac{g_p}{\omega} + g_d\right)\sin\omega\tau,$$
$$\sigma_e = \sigma + \left(\frac{g_p}{\omega} + g_d\right)\cos\omega\tau \tag{35}$$

for $\phi = \dfrac{\pi}{2\omega}$ and

$$\mu_e = \mu + \left(\frac{g_p}{\omega} - g_d\right)\sin\omega\tau,$$
$$\sigma_e = \sigma + \left(\frac{g_p}{\omega} - g_d\right)\cos\omega\tau \tag{36}$$

for $\phi = 3\pi/2\omega$.

As the time-delay τ varies, they can go to the maximum and minimum, respectively,

$$\mu_e = \mu \pm \left|\frac{g_p}{\omega} + g_d\right|, \ \sigma_e = \sigma \quad \text{or} \quad \mu_e = \mu, \ \sigma_e = \sigma \pm \left|\frac{g_p}{\omega} + g_d\right| \tag{37}$$

for $\phi = \pi/2\omega$, and

$$\mu_e = \mu \pm \left|\frac{g_p}{\omega} - g_d\right|, \ \sigma_e = \sigma \quad \text{or} \quad \mu_e = \mu, \ \sigma_e = \sigma \pm \left|\frac{g_p}{\omega} - g_d\right| \tag{38}$$

for $\phi = 3\pi/2\omega$.

It follows from equations (37) and (38) that there are two cases to be considered depending on the quantities of the feedback gains:

Case I: If the feedback is implemented in such a way that $\mu > |g_p/\omega + g_d|$ or $\mu > |g_p/\omega - g_d|$, the resulting μ_e is always positive regardless of the values of the time-delays. The possible combination of the feedback gains is qualitatively shown in Figure 1. If the feedback gains are chosen out of the region shaded by thin lines, the time-delays cannot violate the inequality $\mu_e > 0$. The selection of the feedback gains guarantees the time-delay stability. For the fixed feedback gains, different control purposes can be easily achieved by the appropriate choice of the time-delays. Usually, μ_e should have a larger value in order to improve the control performance.

Figures 2(a) and 2(b) show the variation of μ_e and σ_e with the time-delay τ for three different $\phi = 0{\cdot}0$, $\pi/2\omega$ and $3\pi/2\omega$, respectively, which correspond to two identical and two distinct time-delays in feedback control. Any time-delays are suitable for the feedback control since μ_e is always positive, but not for the optimal control performance. For the cases of two distinct time-delays, μ_e is greater than μ in the region $\tau < \pi/\omega \approx 1{\cdot}05$, while it is

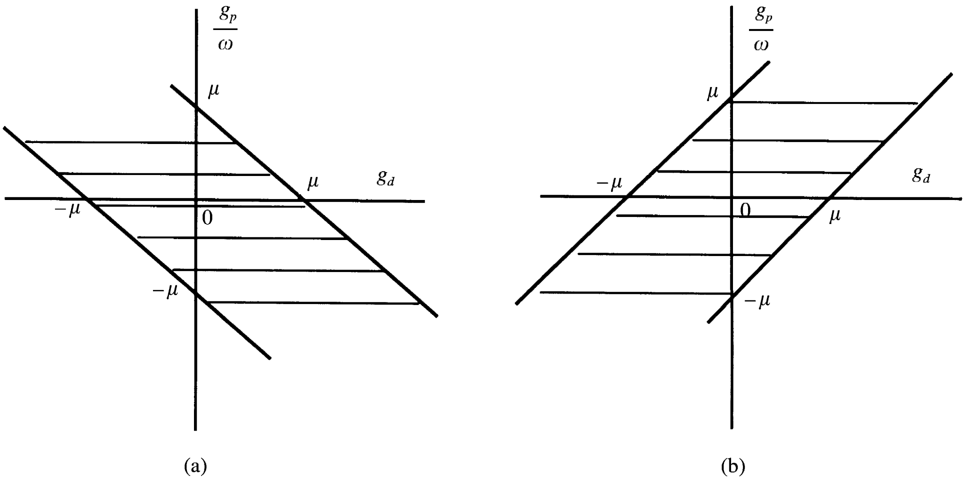

Figure 1. The selection of feedback gains: (a) for $\phi = \pi/2\omega$, (b) for $\phi = 3\pi/2\omega$.

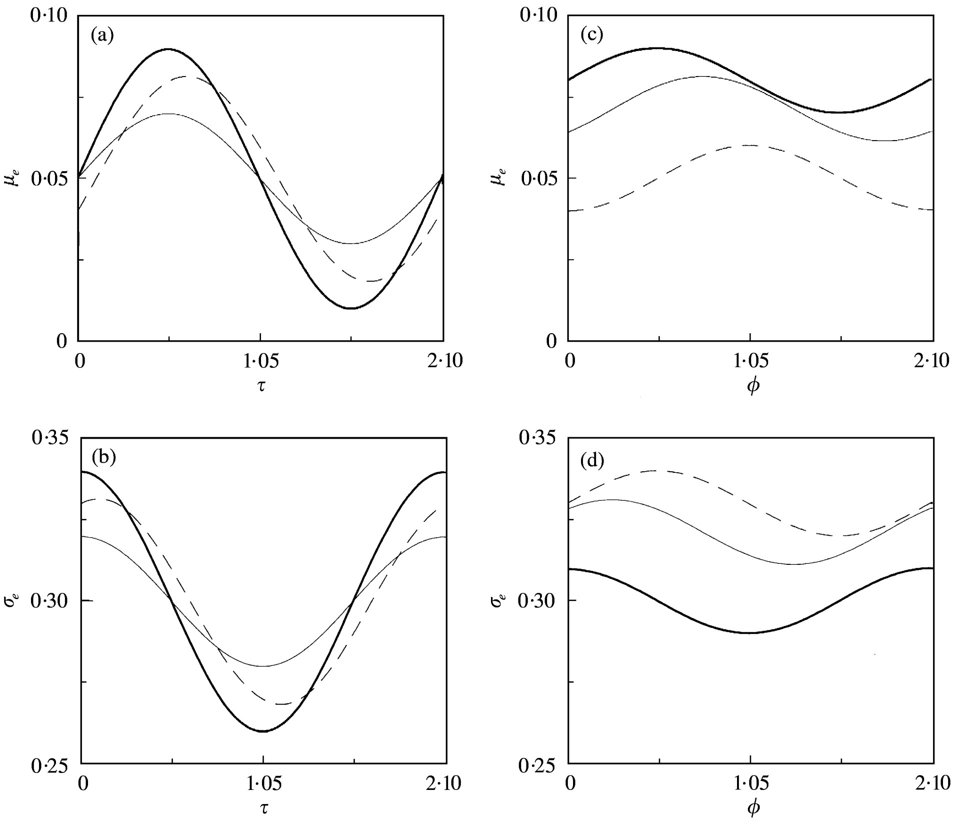

Figure 2. The variation of μ_e and σ_e versus the time-delays for $\mu > |g_p/\omega + g_d|$: (a) and (b) ---- curves are for $\phi = 0{\cdot}0$, —— curves for $\phi = 3\pi/2\omega$, ——— curves for $\phi = \pi/2\omega$; (c) and (d) ---- curves for $\tau = 0{\cdot}0$, —— curves for $\tau = \pi/4\omega$, ——— curves for $\tau = \pi/2\omega$.

smaller than μ in the regime $\tau > \pi/\omega$. The time-delay should be selected from the region $\tau < \pi/\omega$, such that a larger μ_e can be obtained. The difference of two time-delays ϕ also has a great influence on μ_e and σ_e. In Figures 2(c) and 2(d), μ_e and σ_e are plotted as a function of the difference of the two time-delays ϕ, under the three different time-delays $\tau = 0{\cdot}0$, $\pi/4\omega$ and $\pi/2\omega$, which correspond to one time-delay in the derivative feedback, and two distinct time-delays in the feedback control respectively. μ_e gets larger for the case of two distinct time-delays in the feedback control than for the case of only one time-delay in the derivative feedback. This indicates that the control performance for the case of two distinct time-delays is superior to the case of one derivative time-delay feedback. It is also noted that, for the case of two distinct time-delays, μ_e is greater in the region $\phi < \pi/\omega \approx 1{\cdot}05$ than in the region $\phi > \pi/\omega$. Thus, the difference of the two time-delays ϕ should be chosen from the region $\phi < \pi/\omega$, such that a larger value of μ_e can be obtained. When $\tau = \pi/2\omega$ and $\phi = \pi/2\omega$, μ_e reaches the maximum.

Case II: If the feedback gains and time-delays are chosen outside of the thin line region in Figure 1, i.e., $\mu < |g_p/\omega + g_d|$ or $\mu < |g_p/\omega - g_d|$, the resulting μ_e may be positive, zero, or negative, depending on the different values of the time-delays. In practical engineering problem, the last two cases should be absolutely prohibited. The time-delays should be carefully designed so that μ_e is guaranteed to be always positive. No explicit analytical criterion for the selection of the time-delays exists, except numerical simulation methods. Figures 3(a) and 3(b) show the variation of μ_e and σ_e with an increase in time-delay τ for $g_p = 0{\cdot}18$ and $g_d = 0{\cdot}02$, under three different $\phi = 0{\cdot}0$, $\pi/2\omega$ and $3\pi/2\omega$, respectively, which also correspond to the cases of two identical and two distinct time-delays in the feedback control. It is easy to find that there exists one portion of the time-delays when μ_e is negative.

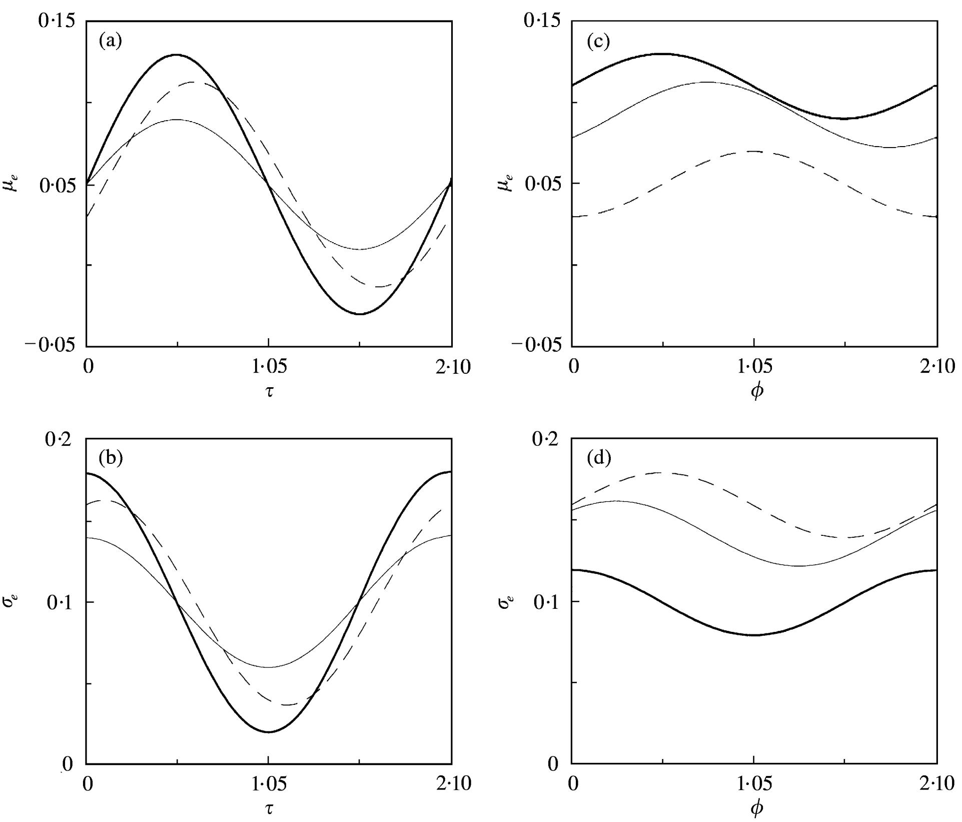

Figure 3. The variation of μ_e and σ_e with the time-delays for $\mu < |g_p/\omega + g_d|$: (a) and (b) ---- curves are for $\phi = 0{\cdot}0$, —— curves for $\phi = 3\pi/2\omega$, ━━━ curves for $\phi = \pi/2\omega$; (c) and (d) ---- curves for $\tau = 0{\cdot}0$, —— curves for $\tau = \pi/4\omega$, ━━━ curves for $\tau = \pi/2\omega$.

From the viewpoint of the feedback control, the time-delays should not be chosen beyond this regime, otherwise the system will be unstable. Under the fixed time-delay $\phi = \pi/2\omega$ and $\phi = 3\pi/2\omega$, the time-delay τ should be selected from the region $\tau < \pi/\omega$. Figures 3(c) and 3(d) illustrate the variation of μ_e and σ_e with an increase in the difference of two time-delays ϕ under three different $\tau = 0{\cdot}0$, $\pi/4\omega$, and $\pi/2\omega$, respectively, which also correspond to the cases of one derivative feedback time-delay and two distinct time-delays in the feedback control. It is also noted that for the cases of two distinct time-delays, μ_e has a larger value for $\tau = \pi/2\omega$, $\phi < \pi/\omega$. When $\tau = \pi/2\omega$ and $\phi = \pi/2\omega$, μ_e attains its largest value. Suitable selection of combination of μ_e and σ_e will be discussed in the next section by some illustrative examples.

4. ILLUSTRATION

This section illustrates the effect of the feedback gains and time-delays on the non-linear dynamical behavior of the controlled system. The results will be presented in a number of figures.

In Figure 4(a), the critical force amplitude f_{crit} is plotted as a function of the time-delay τ for three different fixed ϕ, while the peak amplitude of the primary resonance response a_p versus the time-delay τ is illustrated in Figure 4(b). It is easily noted that f_{crit} and a_p vary

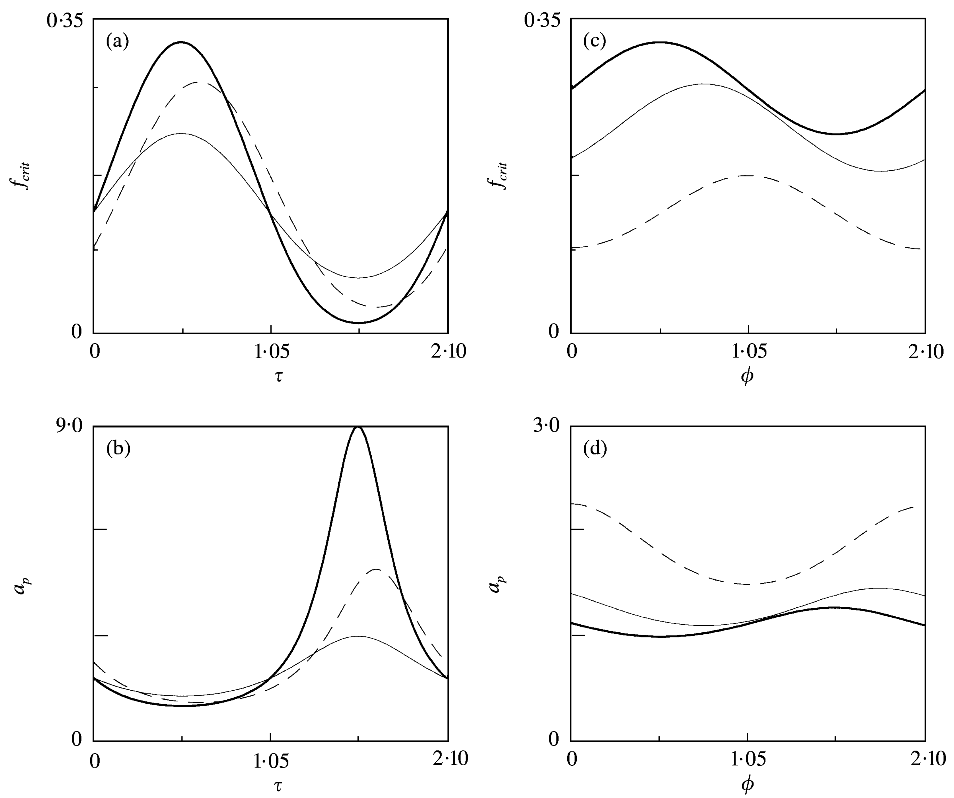

Figure 4. The critical force amplitude f_{crit} and the peak amplitude of the primary resonance response a_p as a function of the time-delays: (a) and (b) – – – – curves are for $\phi = 0{\cdot}0$, —— curves for $\phi = 3\pi/2\omega$, ━━━ curves for $\phi = \pi/2\omega$; (c) and (d) – – – – curves for $\tau = 0{\cdot}0$, —— curves for $\tau = \pi/4\omega$, ━━━ curves for $\tau = \pi/2\omega$.

significantly as the time-delay τ increases. If, unfortunately, the time-delay is not appropriately selected, a smaller μ_e is acquired. Subsequently, f_{crit} reaches a smaller value too, while a_p attains a larger value. This leads to a poor control performance. For the case of two distinct time-delays in feedback control, the time-delay τ should be implemented in the region $\tau < \pi/\omega (\approx 1{\cdot}05)$. Thus, a larger f_{crit} and a smaller a_p can be obtained. For three different fixed time-delays $\tau = 0{\cdot}0$, $\pi/4\omega$ and $\pi/2\omega$, the corresponding f_{crit} and a_p are plotted in Figures 4(c) and 4(d), respectively, as functions of the difference of two time-delays ϕ. It is easy to see that when $\tau = \pi/2\omega$, the critical force amplitude f_{crit} is larger than any other value of the time-delay τ for a fixed ϕ, while a_p has a smaller value. Furthermore, f_{crit} is larger while a_p is smaller in $\phi < \pi/\omega$ than in $\phi > \pi/\omega$. Thus, the difference of two time-delays ϕ should be implemented in the region $\phi < \pi/\omega$ for the purpose of optimal control.

The frequency–response curves (a versus σ) for the primary resonance response are depicted in Figure 5 for three sets of the time-delays. The response curves have an unstable portion for the time-delays $\tau = 0{\cdot}0$, $\phi = 0{\cdot}0$ and $\tau = 0{\cdot}0$, $\phi = \pi/2\omega$, which correspond to the cases of no time-delays and of only one derivative feedback time-delay in the feedback control. In contrast, for two distinct time-delays $\tau = \pi/2\omega$ and $\phi = \pi/2\omega$, no unstable region exists in the system response curve. This indicates that saddle–node bifurcation and jump phenomenon can be eliminated by suitable time-delays. Moreover, the peak amplitude of the primary resonance response a_p for $\tau = \pi/2\omega$ and $\phi = \pi/2\omega$ is smaller than that for the other two cases.

Figure 6 also shows the frequency–response curves for the primary resonance response with $g_p = 0{\cdot}18$ and $g_d = 0{\cdot}02$, under different time-delays. The feedback gains are selected in accordance with Case II discussed in section 3. There exists an interval in which three solutions exist, and jump phenomenon is presented for $\tau = 0{\cdot}0$, $\phi = 0{\cdot}0$ and $\tau = 0{\cdot}0$, $\phi = \pi/2\omega$. In contrast, for $\tau = \pi/4\omega$, $\phi = \pi/2\omega$, there only exists one solution. Jump and hysteresis phenomena do not exist. This simple example also indicates that the saddle–node bifurcation and jump phenomenon can be eliminated by appropriate selection of the time-delays.

For the superharmonic resonance response, the suitable choice of the time-delays and feedback gains can also improve the control performance. Moreover, the occurrence of saddle–node bifurcation, jump and hysteresis phenomena can be delayed or eliminated.

As an illustration, Figures 7(a) and 7(b) show the variation of the critical force amplitude f_{crit} and the peak amplitude of the free oscillation term a_p for $f = 6{\cdot}8$ with the time-delay τ,

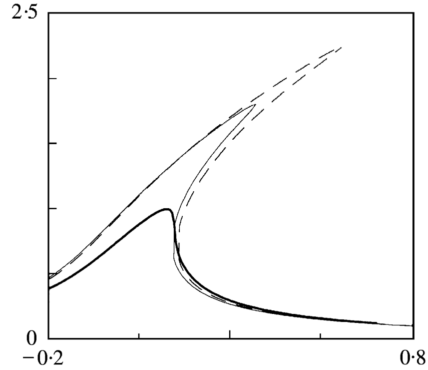

Figure 5. Frequency–response curves for primary resonance for three sets of the time-delays, – – – – curves for $\tau = 0{\cdot}0$ and $\phi = 0{\cdot}0$, —— curves for $\tau = 0{\cdot}0$ and $\phi = \pi/2\omega$, ——— curves for $\tau = \pi/2\omega$ and $\phi = \pi/2\omega$.

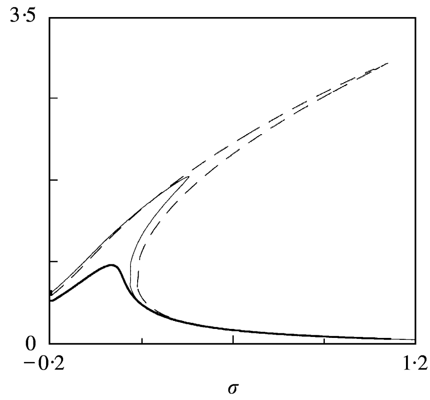

Figure 6. Frequency–response curves for primary resonance for three sets of the time-delays under $g_p = 0{\cdot}18$ and $g_d = 0{\cdot}02$, ---- curves for $\tau = 0{\cdot}0$ and $\phi = 0{\cdot}0$, —— curves for $\tau = 0{\cdot}0$ and $\phi = \pi/2\omega$, ——— curves for $\tau = \pi/4\omega$ and $\phi = \pi/2\omega$.

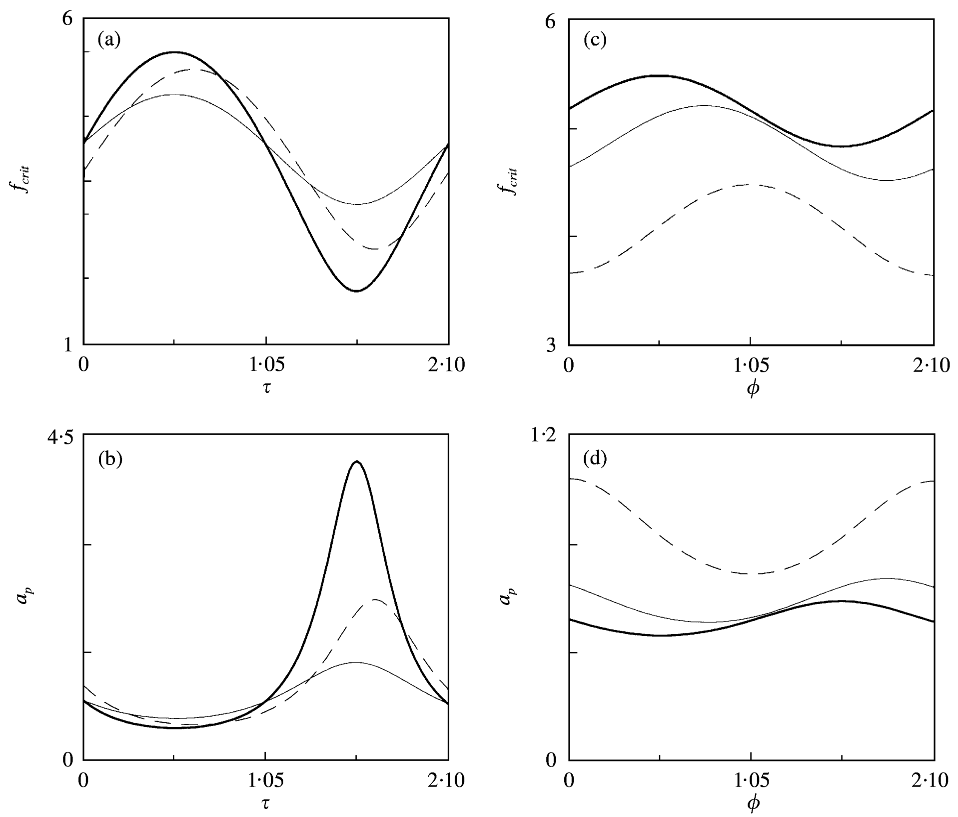

Figure 7. The critical force amplitude f_{crit} for the superharmonic resonance response and the peak amplitude of the free oscillation term a_p as a function of the time-delays: (a) and (b) ---- curves are for $\phi = 0{\cdot}0$, —— curves for $\phi = 3\pi/2\omega$, ——— curves for $\phi = \pi/2\omega$; (c) and (d) ---- curves for $\tau = 0{\cdot}0$, —— curves for $\tau = \pi/4\omega$, ——— curves for $\tau = \pi/2\omega$.

under three different ϕ, $\phi = 0{\cdot}0$, $\pi/2\omega$ and $3\pi/2\omega$ respectively. In contrast, Figure 7(c) and 7(d) demonstrate the variation of f_{crit} and a_p with ϕ for the three different time-delays $\tau = 0{\cdot}0$, $\pi/4\omega$ and $\pi/2\omega$. The feedback gains are implemented in accordance with Case I discussed in section 3. Here, as in the case of primary resonance, the optimal control performance can be achieved by the selection of $\tau < \pi/\omega$ and $\phi < \pi/\omega$.

Figure 8 shows the superharmonic frequency–response curves for three different sets of the time-delays. There exists a region of coexistence of the three solutions for $\tau = 0{\cdot}0$, $\phi = 0{\cdot}0$ and $\tau = \pi/\omega$, $\phi = 3\pi/4\omega$. The bending of the frequency–response curves is responsible for a jump phenomenon. The value of the detuning parameter σ for saddle–node bifurcation is larger for $\tau = \pi/\omega$, $\phi = 3\pi/4\omega$ than that for $\tau = 0{\cdot}0$, $\phi = 0{\cdot}0$. This indicates that the occurrence of saddle–node bifurcation and jump phenomenon can be delayed by certain values of the time-delays. For $\tau = \pi/4\omega$ and $\phi = \pi/2\omega$, there is no jump and hysteresis phenomena. This again suggests that saddle node bifurcation and jump phenomenon can be eliminated by certain values of the time-delays. Thus, the control performance can be enhanced by the optimal selection of the feedback gains and time-delays.

For the subharmonic resonance response, the time-delays can change the regime for the occurrence of subharmonic resonance. Figure 9 shows the regions where subharmonic

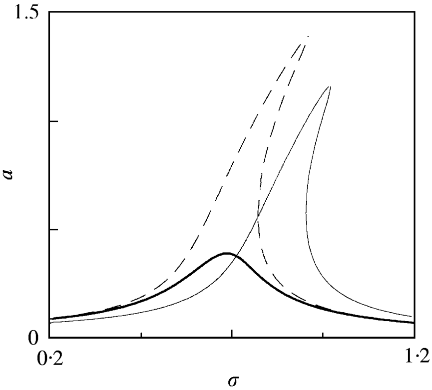

Figure 8. Superharmonic frequency response curves for three sets of the time-delays under $g_p = 0{\cdot}18$ and $g_d = 0{\cdot}02$, ---- curves for $\tau = 0{\cdot}0$ and $\phi = 0{\cdot}0$, —— curves for $\tau = \pi/\omega$ and $\phi = 3\pi/4\omega$, ——— curves for $\tau = \pi/4\omega$ and $\phi = \pi/2\omega$.

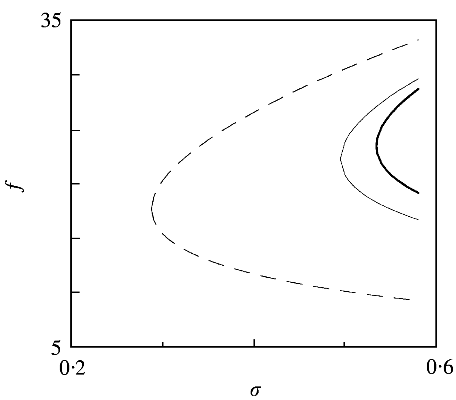

Figure 9. Regions where subharmonic responses exist for three sets of the time-delays: ---- curves for $\tau = 0{\cdot}0$ and $\phi = 0{\cdot}0$, —— curves for $\tau = \pi/4\omega$ and $\phi = 3\pi/2\omega$, and ——— curves for $\tau = \pi/4\omega$ and $\phi = \pi/4\omega$.

response exists for the three different sets of time-delays. It is noted that the regions for the existence of subharmonic responses are different. When no time-delays are implemented in the feedback control (i.e., $\tau = 0{\cdot}0$, $\phi = 0{\cdot}0$), the region is the largest one. For a fixed $\tau = \pi/4\omega$, the region gets smaller at $\phi = 3\pi/2\omega$ and $\phi = \pi/4\omega$. When $\tau = \pi/4\omega$ and $\phi = \pi/2\omega$, subharmonic resonance response does not occur. This indicates that there always exist certain regimes of the time-delays where subharmonic response does not exist.

5. CONCLUSIONS

The non-linear response of a harmonically excited non-linear s.d.o.f. system with two distinct time-delays is investigated under primary, superharmonic, and subharmonic resonances. The effect of the feedback gains and time-delays on the non-linear response of the system is discussed. It is found that an appropriate feedback can enhance the control performance. A suitable choice of the feedback gains and time-delays can enlarge the critical force amplitude, and lessen the peak amplitude of the response (or peak amplitude of the free oscillation term) for the case of primary resonance (superharmonic resonance). Furthermore, a proper feedback can eliminate saddle–node bifurcation, thereby eliminating jump and hysteresis phenomena taking place in the corresponding uncontrolled system. For subharmonic resonance, an adequate feedback can remove or eliminate the occurrence of subharmonic resonance response.

ACKNOWLEDGMENTS

The authors would like to thank the anonymous reviewers for helpful comments and suggestions. This research was supported in part by the City University of Hong Kong, the Key Project Fundation of Educational Committee of Inner Mongolia and by the Natural Science Foundation of Inner Mongolia, P. R. China.

REFERENCES

1. C. R. FULLER, S. J. ELLIOTT and P. A. NELSON 1996 *Active Control of Vibration*. London: Academic Press, Harcourt Brace and Company.
2. W. AERNOUTS, D. ROOSE and R. SEPULCHRE 2000 *International Journal of Bifurcation and Chaos* **10**, 1157–1164. Delayed control of a Moore–Greitzer axial compressor model.
3. R. H. PLAUT and J. C. HSIEH 1987 *Journal of Sound and Vibration* **114**, 73–90. Chaos in a mechanism with the time-delays under parametric and external excitation.
4. R. H. PLAUT and J. C. HSIEH 1987 *Journal of Sound and Vibration* **117**, 497–510. Nonlinear structural vibrations involving a time-delay in damping.
5. J. L. MOIOLA, H. G. CHIACCHIARINI and A. C. DESAGES 1996 *International Journal of Bifurcation and Chaos* **6**, 661–672. Bifurcation and Hopf degeneracies in nonlinear feedback systems with the time-delay.
6. H. Y. HU and E. H. DOWELL and L. N. VIRGIN 1998 *Nonlinear Dynamics* **15**, 311–327. Resonances of a harmonically forced Duffing oscillator with the time-delay state feedback.
7. H. Y. HU and Z. H. WANG 1998 *Journal of Sound and Vibration* **214**, 213–225. Stability analysis of a damped s.d.o.f. system with two time-delays in state feedback.
8. L. PALKOVICS and P. J. Th. VENHOVENS 1992 *Vehicle System Dynamics* **21**, 269–296. Investigation on stability and possible chaotic motions in the controlled wheel suspension system.
9. A. H. NAYFEH 1973 *Perturbation Methods*. New York: John Wiley & Sons.
10. A. H. NAYFEH and B. BALACHANDRAN 1995 *Applied Nonlinear Dynamics*. New York: John Wiley and Sons.
11. A. H. NAYFEH and D. T. MOOK 1995 *Nonlinear Oscillations*. New York: John Wiley.

APPENDIX A: NOMENCLATURE

u	the response of the system
ω	the natural frequency
μ	the damping coefficient ($\mu > 0$)
α	the coefficient of the cubic non-linearity
K	the amplitude of the excitation
Ω	the frequency of the excitation
ε	the small dimensionless parameter
g_p	the proportional feedback control gain
g_d	the derivative feedback control gain
τ_1, τ_2	the time-delays ($\tau_i > 0$)
f	the parameter related to the excitation amplitude
σ	the external detuning
T_n	the time scale
a	the amplitude of the primary resonance response, or the amplitude of the free oscillation term for the super- and subharmonic resonance responses
γ	the phase of the primary resonance response, or the phase of the free oscillation term for the super- and subharmonic resonance responses
a_p	the peak amplitude of the primary resonance response, or the peak amplitude of the free oscillation term for superharmonic resonance response
f_{crit}	the critical force amplitude
λ	the eigenvalue of the corresponding Jacobian matrix
τ	the time-delay
ϕ	the difference of two time-delays